JCTC Journal of Chemical Theory and Computation

On the Catalytic Role of Ge^+ and Se^+ in the Oxygen Transport Activation of N_2O by CO

S. Chiodo, F. Rondinelli, N. Russo, and M. Toscano*

Dipartimento di Chimica and Centro di Calcolo ad Alte Prestazioni per Elaborazioni Parallele e Distribuite-Centro d'Eccellenza MIUR, Universita' della Calabria, I-87030 Arcavacata di Rende (CS), Italy

Received July 25, 2007

Abstract: The different reactivity of two first row cations selenium and germanium, in activating the reduction of nitrous oxide by carbon monoxide, was theoretically investigated at the density functional level using large basis sets and pseudopotential for metal atoms. In the two examined cases, the reaction mechanisms appeared to be quite different. Germanium shows a very good performance as far as thermodynamic and kinetic aspects are concerned. Selenium, experimentally recognized as an inactive catalyst, was instead found potentially able to catalyze the process through a mechanism of spin orbit coupling involving species with doublet multiplicity.

Introduction

Among the main agents of global warming, the long-lived greenhouse gases such as carbon dioxide, methane, nitrous oxide, and halogenated chlorofluorocarbons contribute to an increase in solar radiation estimated as more than 1%. In particular, the N_2O impact toward the environment is even more negative than CO_2 and methane effects because of several factors. The considerable absorption of infrared radiation from the earth by nitrous oxide is due to its persistence in the atmosphere for about 130 years. Moreover, N_2O is so stable to reach the troposphere, where it gives rise to nitric oxide which is responsible for the depletion of the ozone layer. The tropospheric concentration of nitrous oxide has recently increased by about 0.2−0.3% per year. For the next decades more than 80% of primary energy will still be of a fossil nature, so in the near future it will not be easy to reduce N_2O emissions. Many interesting strategies to limit, at least partly, the damages connected to the greenhouse problem were proposed, like a rational use of energy and the improvements in the automobile technology. Nevertheless, the most promising way to reduce the N_2O environmental impact is its catalytic reduction. Recently, experimental measurements carried out by using an inductively coupled plasma/selected-ion flow tube (ICP/SIFT) tandem mass spectrometer, tested the efficiency of many atomic cations to catalyze the activation of nitrous oxide by carbon monoxide.[1−3] While the experimental procedure and the rate coefficients for this kind of O-atom transport reactions are well-known, few theoretical investigations were performed to compute the potential-energy landscapes for the catalytic cycle, illustrated in Scheme 1.

So far, 26 atomic cations were experimentally checked for their catalytic performance.[1]

The elucidation of the processes activation barriers is very attractive because all of them are characterized by an O-atom affinity which should make the catalytic cycle happen, but only ten activate nitrous oxide at room temperature.[1] Therefore, the theoretical study of the PES is the only tool to understand the reason of the cations different catalytic efficiency. In our work, we considered the performance of selenium and germanium monocations. The case of selenium and germanium is very remarkable because, although they belong to the same period, selenium gives rise to a very slow reaction while germanium is the most efficient main group catalyst.

Furthermore, the analysis of the species involved in the mechanism, apart from the elucidation of the catalytic activity, is worthwhile for catalytic bond activation of ions with small molecules.

Computational Strategy

All calculations presented here were carried out using the Gaussian03 suite of programs.[4]

* Corresponding author fax: +39-0984-492044; e-mail: m.toscano@unical.it.

10.1021/ct700184q CCC: $40.75
Published on Web 12/22/2007

Scheme 1. N_2O Activation Cycle by CO in the Presence of Cationic Catalysts

The hybrid nonlocal B3LYP functional,[5,6] the Stuttgart RLC ECP[7] for selenium and germanium, and the 6-311+G-(d) basis set for all other atoms were used to perform complete optimizations of geometries without any constraints. Minima and transition states on the potential energy profiles were determined examining a large number of initial structures and then characterized through vibrational analysis. Minima were connected to the transition state by means of an intrinsic reaction coordinate (IRC)[8] procedure implemented in the Gaussian03 code.

Zero point energy corrections were included in all B3LYP energetic data.

NBO analysis as implemented in the Gaussian03 code[9] was performed to give better insight in the metal ion−ligand bond nature.

For germanium reaction profile, single point energy refinement on the B3LYP 6-311+G(d)/SDD optimized geometries was performed using the QCISD(T)[10] method, an iterative treatment of single and double excitations followed by a noniterative perturbative treatment of triple excitations to fifth order. The QCISD(T) scheme includes the same fifth order terms as the CCSD(T)[11,12] method and shows a very similar performance with it, giving reliable results as far as molecular structure, vibrational frequencies, and energetics are concerned.[13−16]

Since in the case of the selenium catalyzed reaction we were interested also in the spin−orbit coupling (SOC) interaction which lends probabilities to crossovers between doublet and quartet states, a method developed recently by our research group to calculate these SOC contributions[17] using the full Breit-Pauli (BP) operator[18] was applied.

As inherent to the Kohn−Sham approach, this scheme of calculation was originally employed to handle pure and hybrid density functional (DF) monodeterminantal wave functions. The SOC matrix elements are calculated by the formula

$$\langle \hat{H}_{BP}^{SO} \rangle = \langle {}^2\Psi_1 | \hat{H}_{BP}^{SO} | {}^4\Psi_2 \rangle \quad (1)$$

using restricted wave functions. However, due to the monodeterminantal nature of the method, it was possible to produce only one value of the SOC matrix elements. Furthermore, since at the present time, the mentioned procedure requires the use of an all electrons basis set, single point calculations on the involved structure at the crossing point were performed at the B3LYP level employing the DZVP and TZVP basis sets for Se, N, and O[19] atoms, respectively. The structure of the minimum energy crossing point (MECP) was determined employing the methodology developed by Harvey et al.[20]

A crude estimation of the transition probability at the MECP can be done using the Landau−Zener formula[21] which is often used for this purpose.

$$P = 1 - e^{-2\delta}$$

$$\delta = \frac{\pi |H_{ij}^{SO}|^2}{\hbar \nu |\Delta g_{ij}|} \quad (2)$$

Here H_{ij}^{SO} is the SOC matrix element between the electronic states, Δg_{ij} is the difference in the slopes of the two intersecting surfaces at the crossing point, and ν is the effective velocity with which the system is passing through the crossing point that can be calculated from the kinetic theory of gases at 298 K.

This formula can only be used for qualitative treatment, thus we have used the obtained information only to gain insight over the most probable reaction path. Following the Gonzalez-Schlegel algorithm[22] geometry optimization was performed at each point along the reaction path, starting from the saddle point up to the stationary point in the reverse direction. A step size δs (where s denotes the distance along the minimum energy path) of 0.01 Å was used. The gradients of the two surfaces at the crossing point were computed by polynomial interpolation.

Results and Discussion

Before evaluating the influence of the two cations on the kinetic features of the process, we analyzed the reaction path relating to the reduction of nitrous oxide by CO in the absence of any catalyst. In this case, the reactive process to evaluate is the following:

$$N_2O + CO \rightarrow N_2 + CO_2 \quad (3)$$

According to our calculations, the mechanism is characterized by the only activation barrier of 47.6 kcal/mol. The potential energy curve, computed at the same level of theory by Böhme et al., shows an energy barrier of 47.2 kcal/mol.[3] Our investigation highlights that the process is very exothermic. We found a ΔH_0 equal to 86.2 kcal/mol, in agreement with the experimental indication of 87.0 kcal/mol.[23]

Catalyzed reaction potential energy surfaces are illustrated in Figure 1. In this figure, we also reported the spectroscopic term symbols for each species and the relative energy values computed with respect to reactants.

For both selenium and germanium catalysts, the reaction mechanism is summarized as follows

$$M^+ + N_2O \rightarrow M(ON_2)^+ \rightarrow M(ON_2)^+ \text{ TS} \rightarrow MO^+ (+N_2) + \mathbf{CO} \rightarrow OMCO^+ (+N_2) \rightarrow OMCO^+ \text{ TS} + (N_2) \rightarrow MOCO^+ + (N_2) \rightarrow M^+ + CO_2 + (N_2) \quad (4)$$

where M corresponds to Se or Ge. Both cations were first considered in their ground state, ^2P ($4s^2\ 4p^1$) for Ge^+ and ^4S ($4s^2\ 4p^3$) for Se^+ owing to the fact that the first excited states of these ions lie at very high energies. In particular, the Ge^+ ^4P ($4s^1\ 4p^2$) and Se^+ ^2P ($4s^2\ 4p^3$) electronic configurations were found 146.7 and 50.3 kcal/mol above the corresponding ground states.

In mechanism 4, N_2 (in italics) is released when monoxide cation is formed, and, after that, CO (in boldface) is

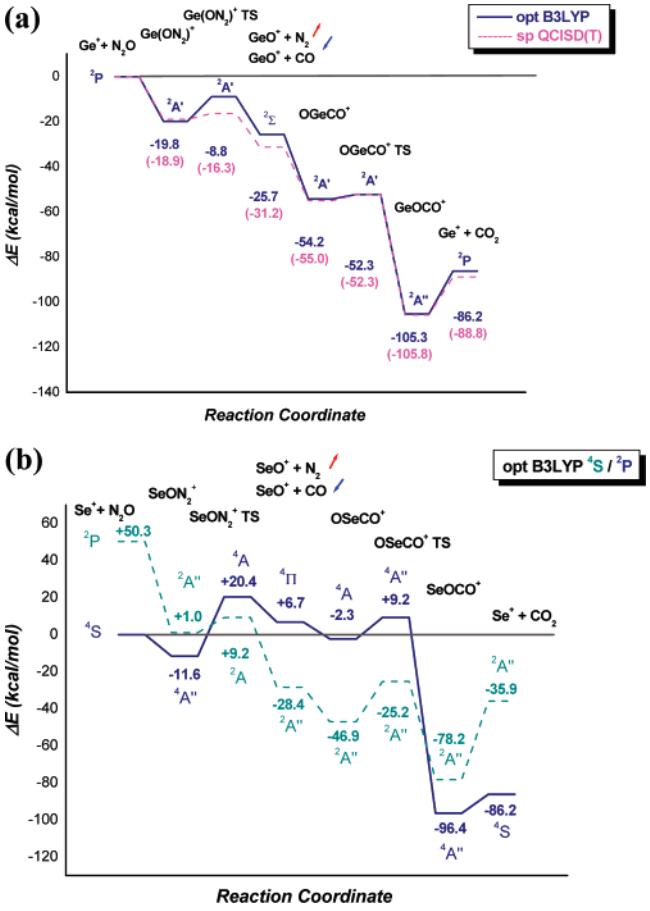

Figure 1. Potential energy surfaces relating to N_2O activation by Ge^+ (a) and Se^+ (b). For Ge^+, solid and dotted lines correspond to the B3LYP and QCISD(T) profiles, while for Se^+ they represent the ground- and excited-state paths, respectively. Blue and red arrows indicate N_2 leaving and CO incoming molecules, respectively.

introduced in the reaction environment. Therefore, the whole process is made up of two steps: MO^+ formation and its coordination to CO until CO_2 is produced and the catalyst is released. Two activation barriers have to be overcome to complete the cycle illustrated in Scheme 1.

Optimized structures for minima and transition states, together with their geometrical parameters, are collected in Figure 2.

In the germanium catalyzed N_2O activation, the first step consists of the coordination of nitrous oxide to the cation. The most favored coordination occurs by the oxygen side. The species $Ge(ON_2)^+$ lies at 19.8 kcal/mol below the reactants asymptote. As it was experimentally proved,[1] GeO^+ does not give rise to N_2O adduct ions. Thus, we excluded the presence of the $Ge(N_2O)^+_n$ species that give rise to the $OGe(N_2O)^+_{n-1}$ compounds. This kind of nitrous oxide multiple coordination was instead observed for other monocations, i.e., for iron.[1,3]

Through an activation barrier of 11.0 kcal/mol, the $Ge(ON_2)^+$ compound evolves in the cation monoxide GeO^+, releasing the inert molecule of N_2.

The imaginary frequency of $Ge(ON_2)^+$ TS, equal to 865 cm^{-1}, corresponds to the stretching of the O−N bond that has to be broken to obtain the nitrogen molecule.

The introduction of carbon monoxide in the reaction environment yields the $OGeCO^+$ adduct lying 54.2 kcal/mol below the reactants. In this species, the coordination of CO to GeO^+ occurs by the metal side. The next minimum $GeOCO^+$, having the CO coordinated from the oxygen side, appears to be more stable to about 3 kcal/mol.

The barrier between the two adducts is very small, as the activation energy corresponds to 1.9 kcal/mol. The imaginary frequency characterizing the $OGeCO^+$ TS, having the value of 165 cm^{-1}, corresponds to the stretching vibrational mode indicating the formation of the new O−C bond and the breaking of the Ge−C bond.

As we observed in our previous studies concerning different metals performances,[24] also for germanium the release of the final products, catalyst and carbon dioxide, is a barrierless step. This finding is not unexpected, as the adduct $GeOCO^+$ shows a linear structure with a quite long metal−oxygen distance (2.272 Å). Besides, the two carbon−oxygen distances are very similar than in the CO_2 free molecule (1.180 and 1.141 Å versus 1.161 Å). Looking at the whole Ge^+ reaction path, in Figure 1(a), the experimental efficiency of the cation in activating nitrous oxide[1] is explained by the fact that the path lies below the reactants asymptote. In fact, what we call the "activation barrier" is not the real barrier of the process in the gas phase. In these conditions there is no possibility for the molecules to lose energy through collisions, so the energy gained in the formation of intermediates is used entirely in the course of reaction.

NBO analysis shows that the bond between the germanium ion and the oxygen atom is ionic in both the $GeON_2^+$ and $GeOCO^+$ species because of the lack of charge transfer from ligand to metal center. This is confirmed by the net charge value on cation (0.96 |e|). On the contrary, this same bond is characterized by a covalent contribution into the GeO^+ and $OGeCO^+$ minima. Into the oxide, a charge transfer of 0.74 |e| occurs from oxygen to germanium ion. The bond originates from the overlap between the two hybrid s(12%)p-(88%) and s(25%)p(75%) orbitals belonging to the germanium ion and oxygen, respectively.

A charge transfer of 0.34 |e| on germanium justifies the presence of a covalent contribution in the Ge−O bond involved in the $OGeCO^+$ system. This bond is due to the overlap of two pure p orbitals. Finally, the NBO analysis suggests that the interaction between germanium ion and carbon atom has an electrostatic nature.

Despite the high energetic difference between the ground and first excited states of Ge^+, we have however ascertained the absence of the two state reactivity phenomenon performing calculations on the stationary points belonging to the most meaningful part (oxide formation) of the quartet pathway, namely the $^4A'$ $GeON_2^+$ and $^4\Sigma$ GeO^+. Results indicated that these species lie at 115.9 and 53.3 kcal/mol above the corresponding doublets confirming the lack of any crossing between the PESs having different multiplicity.

Because of the excellent catalytic performance of germanium, we found interesting to calculate the stationary points energies by the QCISD(T) method.

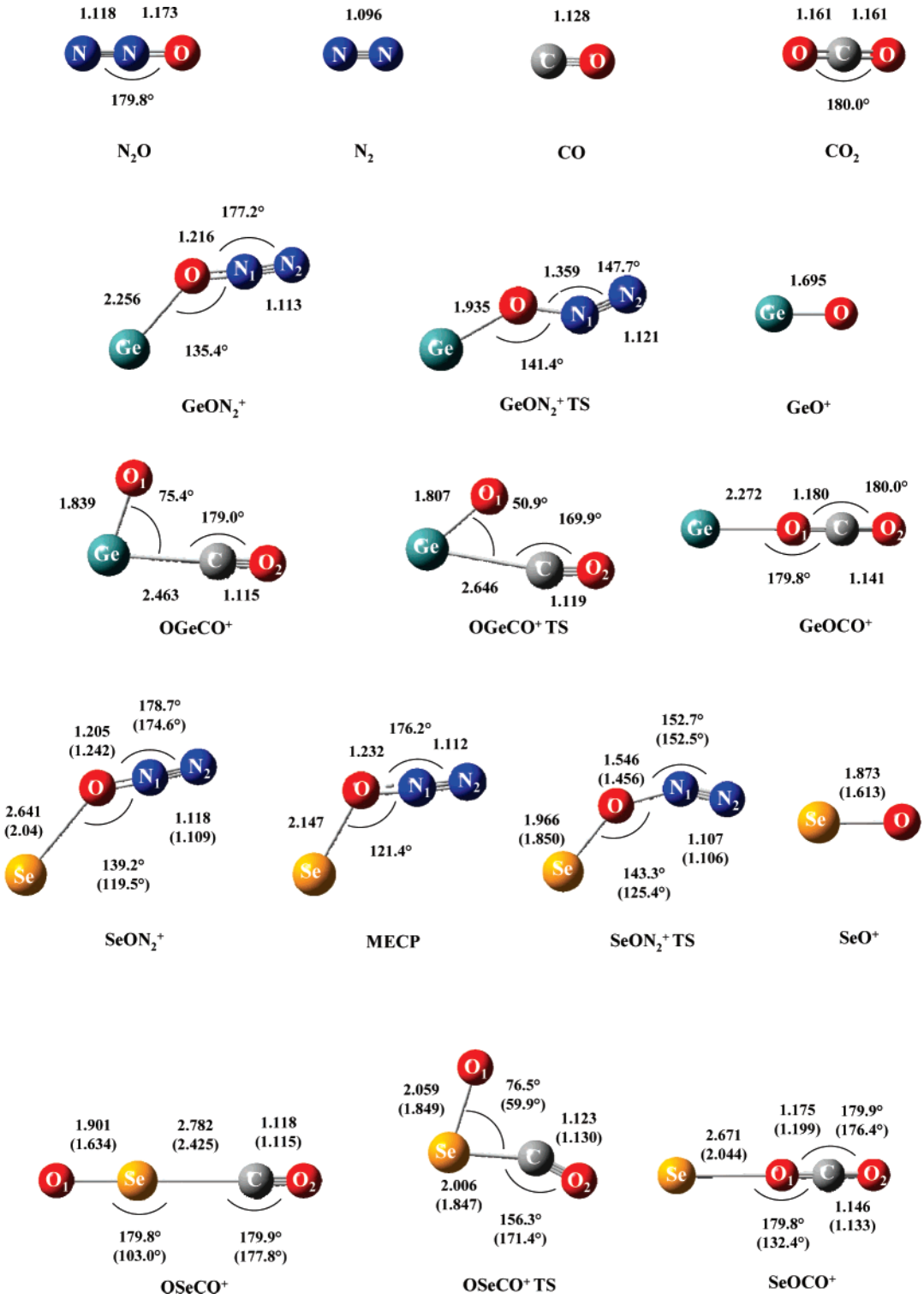

Figure 2. Optimized geometries of species involved in Ge^+ and Se^+ PES. Values in parentheses are referred to selenium adducts in the excited state. Bond lengths are given in Å and angles in deg.

The energetic path obtained at the QCISD(T) level is very similar to the B3LYP one, especially after the oxide formation. In the first part of the profile, the main difference concerns the barrier height to overcome for reaching the GeO^+ species. In fact, it decreases 8.4 kcal/mol with respect to that obtained using the DF approach. However, this does not change the general reaction mechanism. On the other hand, it should be remembered that the QCISD(T) energetic path is the result of a single point computation.

The features of the B3LYP selenium ground state PES, illustrated in Figure 1(b), are completely different than those of germanium. Looking at this reaction path, it seems that Se^+ can give rise only to small amounts of the cation monoxide. Experimentally, because of too small signal intensity SeO^+ presence in the reaction environment was not appreciated by any kind of ICP/SIFT measurement.[1]

In the selenium case, both the activation barriers of the reaction path lie above the reactants asymptote. This indicates

that the reaction is not kinetically favored. The first step consists of the coordination of N_2O to the selenium cation. As for germanium, the most stable adduct resulting from this interaction is characterized by the oxygen−selenium bond, and there is no experimental evidence of other N_2O coordination compounds. The corresponding minimum, $SeON_2^+$, lies at 11.6 kcal/mol below the reactants asymptote.

The coordination to selenium does not substantially change the structure of free N_2O. The N−N distance is exactly the same both in the free molecule and in the $SeON_2^+$ compound (see Figure 2). N_2O is still linear. As a result of the interaction with selenium, we can just note a slight change of the N−N−O angle (179.8° in the free molecule versus 178.7° in the coordination compound).

The detachment of the N_2 molecule involves the overcoming of a considerable activation barrier. In fact, the transition state, indicated in Figure 1(b) as $Se(ON_2)^+$ TS, is located on the PES at 20.4 kcal/mol above the reactants asymptote. This high barrier (32.0 kcal/mol) implies the lack of an appreciable quantity of monoxide cation, as it was experimentally observed. The transition state structure shows, as expected, the increase of the O−N distance that reaches the value of 1.546 Å, while the O−N−N angle assumes the width of 152.7°. The imaginary frequency of 861 cm^{-1} corresponds to the stretching vibrational mode of O−N bond.

The introduction of the carbon monoxide in the reaction environment leads to $OSeCO^+$ formation. Selenium-side CO coordination to the SeO^+ monoxide gives rise to a linear molecule located at 2.3 kcal/mol below the reactants asymptote.

In the next transition state, located at 9.2 kcal/mol above the reactants asymptote, the O−Se−C angle is equal to 76.5°, and the distance between C and O that will form a new bond in the $SeOCO^+$ adduct is 2.520 Å. The imaginary frequency, describing the incoming C−O bond stretching, is 611 cm^{-1}.

As for the other cations we previously studied, the $SeOCO^+$ adduct in which coordination of carbon monoxide occurs by the oxygen side is energetically favored with the respect to the $OSeCO^+$ species. In this case, it lies 96.4 kcal/mol below the reactants energy. $SeOCO^+$ is a linear molecular system in which, as for $GeOCO^+$, the geometrical parameters indicate that the next step does not imply the presence of an activation barrier. In fact, the Se−O distance is 2.671 Å, and the carbon−oxygen bond lengths are very similar than in carbon dioxide molecule (1.146 and 1.175 versus 1.161 Å). Once again, the carbon dioxide detachment is a barrierless step.

The NBO analysis for the species involving selenium ion gives information similar to that obtained for germanium. In particular, the Se−O bond is ionic in the $SeON_2^+$ and $SeOCO^+$ adducts and characterized by a small covalent contribution in the other two minima. The charge transfer from oxygen to selenium ion in the oxide is of about 0.2 |e|. Also in this case, the bond originates from the overlap between two hybrid sp orbitals of the two involved atoms that have a more pronounced p character than in the case of germanium. The covalent bond in the $OGeCO^+$ species is still obtained by the overlap of two pure p orbitals. The net charge on the selenium ion is 0.1 |e|. The Ge−C bond is ionic.

As in the case of the germanium and also for the selenium cation, computations on species lying on the path of the excited state were performed to exclude the existence of crossing between the PESs. $^2A''$ $SeON_2^+$ and $^2A''$ SeO^+ adducts were found at 12.6 above and 35.1 kcal/mol below the corresponding quartets, respectively (see Figure 1(b)), suggesting a greater stability of SeO^+ in the excited rather than in the ground state. The transition state connecting the two examined minima was located at only 8.2 kcal/mol above the $^2A''$ $SeON_2^+$ system. The next doublets $OSeCO^+$ minimum and transition state were found still more stable than the quartets (of 44.7 and 34.4 kcal/mol, respectively). Finally, the last $SeOCO^+$ species and the final products were located at 18.2 and 50.3 kcal/mol above the corresponding ground-state adducts.

These results indicate clearly the presence of two crossings between the profiles at different multiplicities. Actually, on the basis of the new set of data, the reduction of nitrous oxide by carbon monoxide catalyzed by selenium ion becomes possible.

The process should start from the formation of the first $SeON_2^+$ species in the electronic state of the quartet and afterwards proceed on the doublet PES until the $SeOCO^+$ is formed. The second crossing is irrelevant for the reaction kinetics, while the first one changes significantly the conclusions about the performance of selenium as catalysts. In fact, as a consequence of a PES lying almost entirely (see Figure 1(b)) below the reaction asymptote, the real energetic expense for the oxide formation decreases considerably with respect to that required in the quartet case (9.2 versus 20.4 kcal/mol). This means that, although with minor efficiency than germanium, the selenium ion could also be active in catalyzing the reaction. All depends on the probability of the SOC between the doublet and quartet surfaces at the crossing point. For this reason we have retained an interest to evaluate this possibility.

The SOC matrix element was found to be, irrespective of its sign, 1034.35 cm^{-1}. The coupling between $^2A''$ and $^4A''$ is due to the z component of the SOC operator (H_{LzSz}). Coordinates of the $SeON_2^+$ species at the minimum energy crossing point (MECP) geometry are defined in the x,y plane. A large contribution to the orbitals involved in the coupling mechanism arises from p_x and p_y orbitals of selenium which are mainly responsible for the increase in the value of the SOC matrix element. The difference in the slopes of the quartet and doublet curves was found to be of 12.49 kcal/(mol Å), irrespective of its sign. All computed data robustly deliver a value of probability strictly close to one.

Thus one can assert that the selenium ion can work as a catalyst thanks to the two state reactivity phenomenon.

This result appears to be in slight disagreement with experimental determination[1] despite the conclusions of the ICP/SIFT study, as far as the inactivity of selenium cation is concerned, are not so categorical. The authors of this study underline that "for some atomic ions (such as Se^+, Re^+, etc.)

that react slowly there is insufficient information to provide an explanation for their low O-atom transfer reactivity".

We think that some explanation can be derived from our calculations that highlight a significant participation of the excited state of the selenium.

Conclusions

The oxygen transport mechanism from nitrous oxide to carbon monoxide in the presence of Ge^+ and Se^+ catalysts was elucidated at the DFT level. The opposite performances of selenium and germanium, claimed by experimental studies, do not find here complete confirmation.

The whole germanium doublet PES lies below the reactants asymptote, indicating that the reaction is thermodynamically and kinetically favored. The rate determining step, in which a fictitious barrier of 11.0 kcal/mol have to be crossed, is the oxide formation. B3LYP computations exclude any participation of the quartet excited state to the catalytic process.

Very similar conclusions can be derived also from single point QCISD(T) profiles, although some part of the paths suffer from the lack of optimization.

On the basis of results concerning the ground state, the selenium ion appears to be inefficient in catalyzing the reduction of N_2O. In fact, both transient key structures were located above the reactants energy and the rate controlling step, corresponding to the formation of SeO^+ cation monoxide, demands an activation energy of 20.4 kcal/mol. Instead, new very interesting conclusions can be derived from the computations concerning the excited doublet state energetic profile. These show that, in agreement with the presence of a spin orbit coupling at the crossing point of two considered energetic paths, whose probability to occur was computed to be equal to one, the reaction proceeds more easily being now the energetic barrier for the oxide formation of only 9.2 kcal/mol.

However, the general conclusions support the experimental data that indicate in germanium ion a better catalyst than selenium.

Acknowledgment. We gratefully acknowledge the Dipartimento di Chimica, Università della Calabria for financial aid.

References

(1) Blagojevic, V.; Orlova, G.; Böhme, D. K. *J. Am. Chem. Soc.* **2005**, *127*, 3545.

(2) Lavrov, V. V.; Blagojevic, V.; Gregory, K. K.; Orlova, G.; Böhme, D. K. *J. Phys. Chem.* **2004**, *108*, 5610.

(3) Böhme, D. K.; Schwarz, H. *Angew. Chem., Int. Ed.* **2005**, *44*, 2336.

(4) Frisch, M. J.; Trucks, G. W.; Schlegel, H. B.; Scuseria, G. E.; Robb, M. A.; Cheeseman, J. R.; Montgomery, J. A., Jr.; Vreven, T.; Kudin, K. N.; Burant, J. C.; Millam, J. M.; Iyengar, S. S.; Tomasi, J.; Barone, V.; Mennucci, B.; Cossi, M.; Scalmani, G.; Rega, N.; Petersson, G. A.; Nakatsuji, H.; Hada, M.; Ehara, M.; Toyota, K.; Fukuda, R.; Hasegawa, J.; Ispida, M.; Nakajima, T.; Honda, Y.; Kitao, O.; Nakai, H.; Klene, M.; Li X.; Knox, J. E.; Hratchian, H. P.; Cross, J. B.; Adamo, C.; Jaramillo, J.; Gomperts, R.; Stratmann, R. E.; Yazyev, O.; Austin, A. J.; Cammi, R.; Pomelli, C.; Ochterski, J. W.; Ayala, P. Y.; Morokuma, K.; Voth, G. A.; Salvador, P.; Dannenberg, J. J.; Zakrzewski, V. G.; Dapprich, S.; Daniels, A. D.; Strani, M. C.; Farkas, O.; Malick, D. K.; Rabuck, A. D.; Raghavachari, K.; Foresman, J. B.; Ortiz, J. V.; Cui, Q.; Baboul, A. G.; Clifford, S.; Cioslowski, J.; Stefanov, B. B.; Liu, G.; Liashenko, A.; Piskorz, P.; Komaromi, V.; Martin, R. L.; Fox, D. J.; Keith, T.; Al-Laham M. A.; Peng C. Y.; Nanayakkara, A.; Challacombe, M.; Gill, P. M. W.; Johnson, B.; Chen, W.; Wong, M. W.; Gonzalez, C.; Pople, J. A. Gaussian, Inc.: Wallingford, 2004.

(5) Becke, A. D. *J. Chem. Phys.* **1993**, *98*, 5648.

(6) Lee, C.; Yang, W.; Parr, R. G. *Phys. Rev. B* **1988**, *37*, 785.

(7) Miehlich, B.; Savin, A.; Stoll, H.; Preuss, H. *Chem. Phys. Lett.* **1989**, *157*, 200.

(8) Gonzalez, C.; Schlegel, H. B. *J. Chem. Phys.* **1989**, *90*, 2154.

(9) Glendening E. D.; Reed A. E.; Carpenter J. E.; Weinhold F. *NBO 3.0 Program Manual*; Madison, WI, 1995.

(10) Pople, J. A.; Head-Gordon, M.; Raghavachari, K. *J. Chem. Phys.* **1987**, *87*, 5968.

(11) Raghavachari, K.; Trucks, G. W.; Pople, J. A.; Head-Gordon, M. *Chem. Phys. Lett.* **1989**, *157*, 479.

(12) Lee, T. J.; Rendell, A. P.; Taylor, P. R. *J. Phys. Chem.* **1990**, *94*, 5463.

(13) Martin, J. M. L. *J. Chem. Phys.* **1994**, *100*, 8186.

(14) Bartlett, R. J.; Stanton, J. F. *Review of Computational Chemistry*; LipKowitz, K. B., Boyd, D. B., Eds.; VCH: New York, 1994; Vol. V, pp 65−169.

(15) Lee, T. J.; Scuseria, G. E. *Quantum Mechanical Electronic Structure Calculations with Chemical Accuracy*; Langhoff, S. R., Ed.; Kluwer Academic: Dordrecht, The Netherlands, 1994; pp 47−108.

(16) Bartlett, R. J. In *Modern Electronic Structure Theory, Part I, Yarkony*; World Scientific: Singapore, 1995; pp 1047−1055.

(17) Chiodo, S.; Russo, N. *J. Comput. Chem.* In press.

(18) Bethe, H. A.; Salpeter, E. E. *Quantum Mechanics of the One and Two Electron Atoms*; Plenum: New York, 1977.

(19) Godbout, N.; Salahub, D. R.; Andzelm, J.; Wimmer, E. *Can. J. Chem.* **1992**, *70*, 560.

(20) Harvey, J. N.; Aschi, M.; Schwarz, H.; Koch, W. *Theor. Chem. Acc.* **1998**, *99*, 95.

(21) (a) Zener, C. *Proc. R. Soc. London, Ser. A* **1932**, *137*, 595. (b) Zener, C. *Proc. R. Soc. London, Ser. A* **1933**, *140*, 1174.

(22) Gonzalez, C.; Schlegel, H. B. *J. Phys. Chem.* **1990**, *94*, 5523.

(23) Lias, S. G.; Bartmess, J. E.; Liebmann, J. F.; Holmes, J. L.; Levin, R. D.; Mallard, W. G. *J. Phys. Chem.* **1988**, Ref, Data *17*, Suppl 1.

(24) Rondinelli, F.; Russo, N.; Toscano, M. *Inorg. Chem.* **2007**, *46*, 7489.

CT700184Q